Processing Effect on Via Extrusion for Through-Silicon Vias (TSVs) in 3D Interconnects: A Comparative Study of Two TSV Structures

Tengfei Jiang[1], Laura Spinella[2], Jay Im[2], Rui Huang[3] and Paul S. Ho[2]

[1] Department of Materials Science and Engineering and Advanced Materials Processing and Analysis Center (AMPAC), University of Central Florida, Orlando, FL, 32816
[2] Microelectronics Research Center, University of Texas, Austin, TX 78712
[3]Department of Aerospace Engineering and Engineering Mechanics, University of Texas, Austin, TX 78712
E-mail: Tengfei.Jiang@ucf.edu

Abstract

In this paper, processing effects of electroplating and post-plating annealing on via extrusion are investigated. The study is based on two TSV structures with identical geometry but different processing conditions. Via extrusion, stress and material behaviors of the TSV structures were first compared. Electron backscatter diffraction (EBSD) and time-of-flight secondary ion mass spectroscopy (TOF-SIMS) were used to characterize the microstructure of TSVs and the additives incorporated during electroplating. Based on the results, processing effects on via extrusion and its mechanism are discussed, including grain growth, local plasticity, and diffusional creep.

1. Introduction

Three-dimensional (3D) integration is a promising solution to overcome the wiring limit imposed on chip performance, power dissipation and package form factor beyond the 14nm technology node [1,2]. In 3D integration, thin dies are connected vertically by Cu through-silicon vias (TSVs). The fabrication of TSVs typically involves deep-etching of via holes, deposition of oxide liner, diffusion barrier, and seed layers, electroplating of Cu for via fill, and then chemical-mechanical planarization (CMP) [3]. Due to the large thermal expansion mismatch between copper (Cu) vias and silicon (Si), complex stresses are induced in and around the TSVs [4]. This can lead to Cu extrusion or TSV "pop-up", which is a serious reliability issue since the vertical protrusion of Cu can cause failure in the adjacent interconnect structures during fabrication or thermal cycling [5-7].

Several mechanisms, including grain growth, dislocation glide, and diffusional creep, can result in irrecoverable protrusion of Cu vias during thermal cycling [8-10]. The microstructure of Cu plays an important role in via extrusion. For example, correlation between grain size and yield strength has been shown to affect plasticity of Cu, and grain boundary diffusion was found to directly correlate to via extrusion [10,11]. Processing conditions, including electroplating and post-plating annealing, are important in controlling the microstructure of Cu vias. Eventually, improving via extrusion reliability requires microstructure control through optimized processing conditions.

2. Test structure

Two sets of TSV structures, referred to as TSV-A and TSV-B, were used in this study. Both structures consisted of blind vias of 5.5×50μm (diameter×height) and Si thickness of 760μm. Different electroplating conditions were used to fabricate TSV-A and TSV-B, although detailed information on electroplating used in the fabrication was not available. In the as-received state, TSV-A wafer was subjected to post-plating annealing at 430ºC for 10min prior to CMP while no post-plating annealing was performed on TSV-B wafer.

Both TSV structure were subjected to a single thermal cycling to 400ºC and the resulting via extrusion was examined by atomic force microscopy (AFM). The height profiles were compared with the as-received vias, i.e. vias without subjecting to thermal cycling. The extrusion profiles extracted across the top of the vias are distinctly different as shown in Fig. 1.

3. Thermo-mechanical and materials characterization

3.1. Substrate curvature measurement

Substrate curvature measurement was performed on both TSV structures to obtain the general thermo-mechanical behavior of the Cu vias. Details of the technique have been described elsewhere [12]. Distinct differences were observed when both TSV structures were subjected to three thermal cycles to 400ºC (Fig. 1). The curvature of TSV-A was nearly linear elastic throughout the thermal cycles. TSV-B, on the other hand, showed large relaxation in the first half-cycle during heating, which was followed by small but observable nonlinearity during cooling of first cycle and subsequent cycles.

Isothermal measurements were carried out where the as-received samples were heated to 400ºC and held for 1 hour before cooling to room temperature. The curvature changes as a function of time (t) were plotted in Fig. 3, where the curvatures at time t=0 were shifted to the same point for comparison. In comparison, TSV-A had minimal curvature relaxation while TSV-B showed significantly larger curvature change at 400ºC, indicating the presence of diffusional creep in TSV-B.

3.2. Microstructure analysis

Microstructure analyses were conducted by EBSD for vias subjected to single temperature cycling tests to 100, 200, 300,

and 400ºC (Fig. 4). No apparent grain growth was seen in TSV-A, indicating a stabilized grain structure. In contrast, significant grain growth occurred in TSV-B, especially beyond 200ºC.

Based on EBSD, the percentages of Σ3 and Σ9 boundaries in both vias were analyzed (Table 1). The amount of twin boundaries was larger in TSV-A than in TSV-B in both the as-received state and after thermal cycled to 200ºC and 400ºC. There appeared to be no systematic change in the amount of twin boundaries with increased thermal cycling temperatures.

3.3. TOF-SIMS

TOF-SIMS was performed to measure the additive elements incorporated in Cu vias during electroplating. For both as-received samples and samples after thermal cycling to 400ºC, the measurements were conducted on via cross-sections. The amount of Cl^-, F^-, S^-, and CN^-, elements commonly found in electrodeposited Cu [13], were normalized to the amount of Cu^- and summarized in Table 2. It should be pointed out that such quantitative comparison was valid only when the Cu matrix was identical in all samples [14]. The measured additive concentration could be affected by the electroplating conditions and the non-uniform distribution of additive elements in the via, depending on where the cross-section was cut through the via. Such comparison should be regarded as semi-quantitative.

4. Discussion

4.1 TSV-A vs. TSV-B

TSV-A and TSV-B have identical geometries but different processing conditions, which were responsible for their distinct extrusion behaviors. There was no apparent via extrusion for TSV-A and its surface profile after thermal cycling was very similar to the reference via, except for slightly increased surface roughness near grain boundaries. The depression at the top surface in Fig. 1a was probably due to dishing effect induced by CMP. In contrast, large via extrusion was observed for TSV-B. The extrusion was non-uniform across the via surface, with hillocks and large height variations relating to grain structure at the via top. The highest extrusion reached as high as 200 nm. The difference in via extrusion was reflected in the curvature measurement as well. In Fig. 2, the curvature of TSV-A was linear elastic, suggesting the absence of inelastic processes during thermal cycling. In comparison, significant curvature relaxation was seen in TSV-B, indicating the presence of inelastic processes causing via extrusion.

4.2 Effect of electroplating

TOF-SIMS showed that for TSV-A, the amount of Cl^-, F^-, S^-, and CN^- elements were comparable before and after thermal cycling, indicating limited out-diffusion of additives. For TSV-B, the amount of additive elements decreased after thermal cycling, which could be related to the out-diffusion of additive species during grain growth [15]. Thus it appeared that TSV-A incorporated much more additive elements than TSV-B during fabrication. Although the detailed difference in electroplating bath chemistry and current density between TSV-A and TSV-B were not available, the different conditions used in the fabrication of the two TSV structures apparently affected the microstructure of Cu in the via. As shown in table 1, TSV-A has significantly larger percentage of twin boundaries than TSV-B. In Cu, it is known that cohesive twin boundaries, especially ∑3 boundaries, have significantly smaller diffusivity than high angle boundaries [16]. With fewer twin boundaries, mass transport via grain boundary diffusion would be more in TSV-B than in TSV-A. This was confirmed by isothermal measurement in Fig. 3, where large curvature relaxation was seen for TSV-B. This in turn contributed to the larger extrusion in TSV-B. Similar observation was reported in a recent study, where smaller extrusion was observed for vias with larger portion of twin boundaries [11].

4.3 Effect of post-plating annealing

Post-plating annealing is known to stabilize grain structure, which was desirable for suppressing via extrusion [8]. This was the case for TSV-A, where no apparent grain growth was observed. Since TSV-B was not subjected to post-plating annealing, grain growth had occurred during thermal cycling and contributed to via extrusion. In a follow-up study, an as-received TSV-B wafer was annealed at 430ºC for 10min in Ar, which was the same condition used for TSV-A. The TSV sample after annealing was called TSV-B annealed. Afterwards, the same thermal cycling and isothermal measurements as described in section 3.1 were performed, and the results were shown in Fig. 5. EBSD and extrusion measurements were also conducted.

Comparing to the as-received sample, the annealed TSV-B sample showed smaller amount of curvature relaxation, both in thermal cycling and isothermal measurements. However, annealing did not eliminate the nonlinear curvature in Fig. 5a, suggesting some inelastic processes were still present. In particular, in the 2nd and 3rd cycles, hysteresis loops had formed, which was evidence of plastic deformation in the Cu vias [17]. In Fig. 5b, the amount of curvature relaxation in the annealed TSV-B sample was smaller than the as-received TSV-B sample but larger than TSV-A, indicating the presence of diffusional creep. On the other hand, EBSD showed no apparent grain growth after thermal cycling and the percentage of twin boundaries were similar to that in Table 1. Although the grain size appeared to have been stabilized after annealing, there was via extrusion after a single thermal cycle to 400ºC with reduced magnitude of around 60 nm. These results suggested that post-plating annealing alone was not effective to eliminate via extrusion.

4.4 Effect of processing on via extrusion

Electroplating and post-plating annealing were the two major factors in the fabrication of the two TSV structures with different via extrusions. Electroplating appeared to be more important than post-plating annealing. Without an optimized electroplating condition, post-plating annealing alone does not seem to be sufficient to eliminate via extrusion. Ideally, optimized processing condition would lead to an optimal microstructure similar to that of TSV-A with stabilized grain structure and large amount of twin boundaries to suppress the inelastic processes and control via extrusion.

5. Summary

In this study, two TSV structures with different processing conditions were compared. The effect of electroplating and post-plating annealing on via extrusion was examined based on the inelastic processes during thermal cycling. The results show that

electroplating and post-plating annealing play important but different roles in controlling via extrusion. These conditions need to be optimized during the fabrication of TSVs to minimize via extrusion.

Acknowledgement

This work was supported by Semiconductor Research Corporation.

References

[1] K. Banerjee et al., *Proc. IEEE*, 89, 5, 602-633 (2001).
[2] J.U. Knickerbocker et al., *IBM J. Res. Dev.*, 52 (6), 553-569 (2008).
[3] P. Garrou et al., *Handbook of 3D Integration*, 2008.
[4] T. Jiang et al., *MRS Bulletin*, 40 (3), pp. 248-256 (2015).
[5] J. Van Olmen et al., *Microelectron Eng.*, **88**, 5,745-748 (2011).
[6] S. Kang et al., *Proc. IEEE 3DIC*, pp. 1-4 (2012).
[7] Y. Li et al., Proc. IRPS, pp. 3E.1.1-3E.1.5 (2014).
[8] J. De Messemaeker et al., *Proc. ECTC*, pp. 586-591, (2013).
[9] T. Jiang et al., *Appl. Phys. Lett.*, **103**, 211906 (2013).
[10] J. De Messemaeker et al., *Proc. ECTC*, 613-619, (2014).
[11] T. Jiang et al., J. Microelectronics and Electronic Packaging, 12 (3), 2015.
[12] T. Jiang et al., Microelectron. Reliab.,53, 53–62 (2013).
[13] P.M. Vereecken et al., *IBM J. Res. Dev.* 49(1), 3-18 (2005).
[14] T. Elko-Hansen et al., The Journal of Physical Chemistry Letters, 5 (7), 1091-1095 (2014).
[15] J.M.E. Harper et al., *J. Appl. Phys.*, 86, 2516-2525 (1999).
[16] L. E. Murr, *Interfacial phenomena in metals and alloys*, 1975.
[17] D. Gan et al., *J. Appl. Phys.*, 97 (10), 103531 (2005).

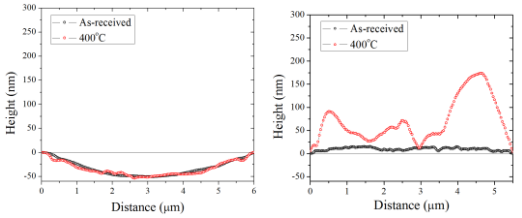

(a) (b)

Figure 1. Height profile across the via diameter for (a) TSV-A and (b) TSV-B

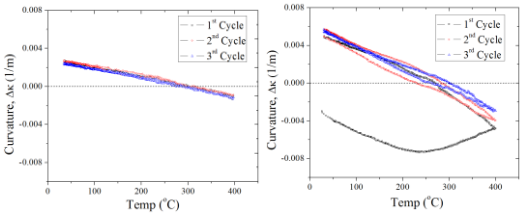

(a) (b)

Figure 2. Curvature-temperature behaviors of (a) TSV-A and (b) TSV-B after thermal cycling to 400ºC for three times.

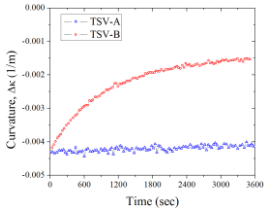

Figure 3. Isothermal relaxation measurement at 400ºC for TSV-A and TSV-B.

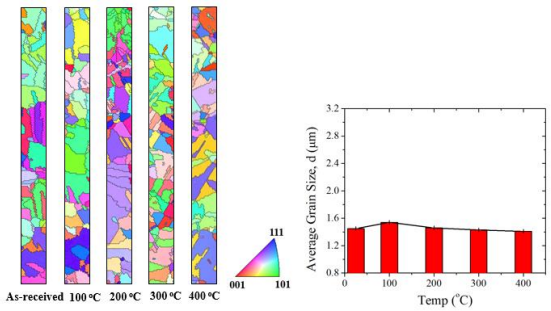

(a)

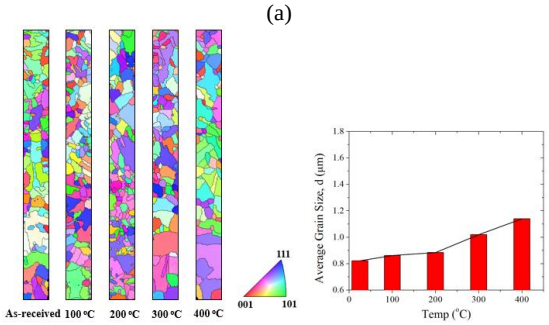

(b)

Figure 4. EBSD grain orientation map and grain size for (a) TSV-A and (b) TSV-B.

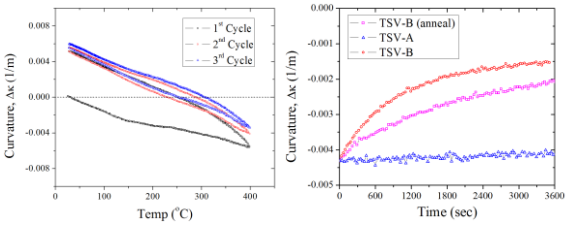

(a) (b)

Figure 5. (a) Curvature-temperature behavior and (b) isothermal relaxation measurement at 400ºC for TSV-B after annealing at 430ºC for 10min in Ar.

Table 1. Percentage of Σ3 and Σ9 boundaries in the as-received and thermal cycled vias for TSV-A and TSV-B.

	As-received (%)		200ºC (%)		400ºC (%)	
	TSV-A	TSV-B	TSV-A	TSV-B	TSV-A	TSV-B
Σ 3	77.4	55.5	71.6	63.8	79.9	60.7
Σ 9	11.4	10.9	9.1	9.3	7.8	8.7
Total	88.7	66.4	80.7	73.1	87.7	69.4

Table 2. Counts of Cl^-, F^-, S^-, and CN^- elements in the TSV.

Counts / Element	TSV-A		TSV-B	
	As-received	400ºC	As-received	400ºC
Cl^-	337.6	334.1	1.26	0.26
F^-	147.2	213.5	10.9	4.63
S^-	7.3	10.8	0.60	0.15
CN^-	114.3	87.2	0.61	0.30